Proapoptotic Function of the Nuclear Crk II Adaptor Protein†

Bishnupriya Kar,‡ Charles T. Reichman,‡ Sukhwinder Singh,‡ J. Patrick O'Connor,§ and Raymond B. Birge*,‡

Department of Biochemistry and Molecular Biology and Department of Orthopedics, UMDNJ—New Jersey Medical School, 185 South Orange Avenue, Newark, New Jersey 07103

Received March 16, 2007; Revised Manuscript Received June 6, 2007

ABSTRACT: Crk II and Crk L have both cytosolic and nuclear functions. While Crk L is a bona fide nuclear signaling protein because of its ability to bind tyrosine-phosphorylated STAT5 and act as a transcriptional coactivator, the function of nuclear Crk II is less well understood. The present study was undertaken to investigate whether Crk II is in the nucleus, how Crk II translocates into the nucleus, whether it possesses a functional NES, and to determine if nuclear Crk II affects cell cycle checkpoints and promotes apoptosis. Toward this goal, we used several independent techniques to show that a significant percentage of the total endogenous Crk II partitions in the nucleus in mammalian cells, where it forms distinct complexes with DOCK180, Wee1, and Abl. We found no evidence that Crk II bound to Crm1 nor that the localization of GFP-Crk II was sensitive to LMB, an inhibitor of Crm1. To better define the significance of nuclear Crk II localization, we generated a GFP-Crk II protein (GFP-Crk-nuc) fused to three tandem nuclear localization signals derived from the SV40 large T-antigen. GFP-Crk-nuc exhibited exclusive nuclear localization, and in contrast to wild-type Crk, GFP-Crk-nuc expressing cells could not be propagated upon selection in G418-containing media, suggesting nuclear accumulation of Crk II caused either growth arrest or apoptosis. When transiently transfected cells were FACS sorted, GFP-expressing cells showed defective cell adhesion on tissue culture surfaces and showed an increased level of apoptosis assessed by pycnotic nuclei, annexin V staining, and PARP cleavage. Although we found that Crk II bound to the cell cycle protein Wee1, expression of GFP-Crk-nuc did not induce a G2/M cell cycle block or cause increased Cdc2 Tyr15 phosphorylation. Finally, upon UV stimulation, we found that endogenous Crk II translocated to the nucleus and potentiated the extent of UV-inducible apoptosis after 4 h. These data suggest that nuclear compartmentalization of Crk II antagonizes its cytoskeletal functions and assign a proapoptotic role to the nuclear pool of Crk II.

Crk[1] is a member of a family of adaptor proteins composed of SH2 and SH3 domains that assemble protein−protein interactions and have important functions in signal transduction downstream of tyrosine kinases (*1*). The Crk II gene was originally identified as an oncogene product, v-Crk or Gag-Crk, encoded by the avian retrovirus CT10 (*2*) and later in an independent isolate of the ASV retrovirus (*3*). Subsequently, two ubiquitously expressed splice variants of cellular *crk* have been characterized, called Crk I and Crk II. Crk II is the longer protein while Crk I has a truncated SH3(C) and a SH3−SH3 linker, and functions like v-Crk (*4*, *5*). Crk-like (Crk L) is encoded by a gene distinct from Crk II, is structurally most similar to c-Crk II, and shows similar SH2 and SH3 binding specificity (*6*), although Crk L is expressed predominantly, but not exclusively, in hematopoietic cells. Biochemical and knockout studies indicate that Crk II and Crk L have only partially overlapping functions, since single knockouts only display partial compensation (*7*, *8*).

The signal transduction functions of v-Crk, Crk I, Crk II, and Crk L have been extensively studied and attributed mainly to the SH2 and first SH3 domain, Crk SH3(N). The Crk SH2 domain binds short phosphotyrosine- (pTyr-Asp-His-Pro-) containing motifs (*9*) in target proteins whereas the N-terminal SH3 domains bind canonical proline-rich motifs with the minimal consensus of Pro-x-x-Pro-x-Lys (*10*). Much attention has been given to the p130^{cas}/HEF family of scaffold proteins (*11*) in Crk signaling because p130^{cas} becomes tyrosine phosphorylated by numerous extracellular matrix molecules and growth factors and hormones, and the central substrate-binding region contains 12−15 multiple tandem pYDHP motifs that when phosphorylated bind Crk (*12*). As such, separate molecular complexes that involve p130^{cas}/Crk/DOCK180, p130^{cas}/Crk/C3G (*13*−*15*), p130^{cas}/Crk/Abl (*16*), and p130^{cas}/Crk/JNK (*17*−*20*) can allow for extraordinary diversity following Crk binding. p130^{cas}/Crk-mediated signaling is implicated in the activation of GTPases such as Rac1, R-Ras, and Rap-1 (*21*, *22*), as well as serine/threonine kinases such as JNK, MKK4, and ERK1/2 (*20*). Collectively, these impinge on multiple aspects of migration, proliferation, and antiapoptotic signaling pathways. However, it is also apparent that Crk proteins are

† This work was supported by NIH Grant GM55760 and a UMDNJ foundation grant to R.B.B. B.K. was funded by a predoctoral fellowship from the New Jersey Commission of Cancer Research.

* To whom correspondence can be addressed. Tel: 973-972-4497. Fax: 973-972-5594. E-mail: birgera@umdnj.edu.

‡ Department of Biochemistry and Molecular Biology, UMDNJ—New Jersey Medical School.

§ Department of Orthopedics, UMDNJ—New Jersey Medical School.

[1] Abbreviations: Crk, CT10 regulator of kinase; LMB, leptomycin B; TNF-α, tumor necrosis factor-α; SV40, Simian virus 40; GFP, green fluorescent protein.

10.1021/bi700537e CCC: $37.00
Published on Web 09/01/2007

not simply conduits for the aforementioned pathways but clearly control the amplitude of signaling. Forced overexpression of Crk in cells increases $p130^{cas}$ tyrosine phosphorylation promoting an intracellular loop that enhances motility and aggressive metastatic behavior of tumor cells (*23*−*25*). A number of recent reports indicate that Crk may indeed be upregulated in human tumors (*26*), including human synovial tumor cells and lung cancer cells (*27*). Studies by Tanaka and colleagues have shown that downmodulation of Crk II by siRNA suppresses cell motility and tumor metastasis, suggesting that Crk may be an important therapeutic target to block the metastatic potential of highly motile cells (*27*, *28*).

Both Crk II and Crk L are regulated by native autoinhibitory phosphorylation events that block the ability of Crk to function as an adaptor protein. Phosphorylation of Tyr221 (in Crk) or Tyr207 (in Crk L) by Abl and Arg family nonreceptor tyrosine kinases causes intramolecular binding of the linker region to the Crk SH2 domain, sequestering the SH2 and SH3(N) from binding in trans to target proteins (*29*), whereas PTP-PEST decreases Crk phosphorylation and promotes cell migration (*30*). Klemke and colleagues were the first to posit that c-Abl-mediated Crk Tyr221 phosphorylation may act as a "molecular switch" to dissociate the $p130^{cas}$, Crk II, DOCK180 ternary complex (*25*). They showed that Crk Tyr221 phosphorylation correlated with decreased aggressive migratory behavior of pancreatic cancer cells and induced apoptosis by blocking Rac1 activation. Similarly, in human breast cancer cells, EphB4 activation results in Abl activation and Abl-inducible Crk II Tyr221 phosphorylation associated with inhibition of cell migration and MMP4 expression (*31*).

In recent years, both Crk II and Crk L have been implicated in nuclear signal transduction events (*32*). For Crk L, elegant studies have shown that Crk L binds tyrosine-phosphorylated STAT5 in Bcr-Abl expressing cells and in a variety of cytokine-stimulated hematopoietic cells (*32*−*37*). In each of these cases, the complex translocates to the nucleus to bind STAT5-responsive elements. Although Crk II can also bind to STAT5, this complex does not appear to enter the nucleus, nor does anti-Crk II antisera supershift STAT5 DNA binding complexes (*35*). Although further studies are required to understand the function of Crk II-STAT5 complexes, these data suggest that Crk II and Crk L have distinct nuclear functions after binding STAT5. On the other hand, interesting studies by Kornbluth and colleagues indicate that Crk II may actively and directly participate in apoptosis in *Xenopus* studies by activating caspases (*38*, *39*). Depletion of Crk II from egg extracts prevented apoptosis, and these studies further demonstrated that Crk binds to the cell cycle regulatory protein Wee1, implying this proapoptotic function of Crk II may be due to nuclear localization (*40*, *41*). Evidence in support of this model includes the fact that Crk II has a putative NES in the C-terminal SH3 domain that when mutated increases cell death and that ionizing radiation increases complex formation between Wee1 and Crk II (*41*). Recent structural studies with Crk L indicate that the Crk NES may only function in the dimeric state of the protein, mediated by a homotypic interaction in the SH3(C) domains (*42*). These studies predict that the Crk II NES motif may become "exposed" conditionally under certain circumstances, an event that would actively promote efflux of a nuclear Crk II pool into the cytoplasm. However, the presence of an NES sequence in Crk II does not explain how Crk II initially traffics to the nucleus since Crk II does not appear to possess any NLS sequences.

Although several studies have posited a bona fide nuclear signaling role for Crk L, in contrast, the regulatory events surrounding Crk II nuclear localization are less well understood. In this study, we used several independent techniques to show that a significant percentage of the total endogenous Crk II partitions into the nucleus in mammalian cells, where it forms distinct Crk complexes with DOCK180, Wee1, and Abl. Generating a nuclear targeting cassette for Crk by fusing tandem SV40 large T-antigen nuclear localization sequences, we achieved durable and persistent targeting of Crk II to the nucleus. GFP-Crk-nuc-expressing cells antagonize cytoplasmic Crk II function by showing decreased adhesion on tissue culture surfaces and inducing spontaneous apoptosis. The translocation of Crk II to the nucleus appears to be dependent, in part, on proteins that bind to the SH3(N) domain, and under the conditions studied in this paper, we found no evidence for a functional NES as evident from binding studies with Crm1 or by virtue of leptomycin B (LMB) sensitivity. Our present data suggest that the nuclear pool of Crk II antagonizes both the proadhesion/migration and the prosurvival functions of Crk II, and in concurrence with the ideas of Kornbluth and colleagues, we posit that nuclear shuttling of Crk II may govern a proapoptotic/prosurvival switch to fine-tune signals for cellular growth, migration, and apoptosis. These studies also reemphasize the importance of subcellular compartmentalization in signal transduction outcomes.

MATERIALS AND METHODS

Cell Culture and DNA Transfection. HEK 293T and HeLa S3 cells were maintained in Dulbecco's modified Eagle's medium [DMEM (Cellgro); 4.5 g of glucose/L with L-glutamine] supplemented with 10% fetal calf serum (Sigma). NIH 3T3 cells were maintained as above except they were cultured in 10% bovine calf serum. MCF-7 cells were grown in DMEM supplemented with 10 μg/mL insulin and 10% FBS. HEK 293T cells were transfected with lipofectamine (Invitrogen), NIH 3T3 cells with lipofectamine2000 (Invitrogen), and HeLa S3 cells with LT1 transfection reagent (Mirus) as per manufacturers' protocols.

Antibodies. Antibodies for Crk II, tubulin, and actin were purchased from Sigma. Antibodies for PARP (H250), myc (9E10), GST (Z-5), Crm1 (H-300), and Wee1 (C-20) were purchased from Santa Cruz Biotechnology. The antibody for phosphohistone H3 was purchased from Upstate Biotechnology. Anti-Crk RF51 antisera (raised against the SH2 domain of Crk) have been previously described (*5*).

Plasmids and Reagents. The plasmid encoding GFP was from Clontech. pEGFP-nuc and pEGFP-nuc-nes were constructed by ligating sequences from the SV40 large T-antigen and PKI (PKR inhibitor). pEGFP-p53-K302N plasmid was a gift from Dr. Horinouchi, University of Tokyo, Japan. pCDNA myc Wee1 was a gift from Dr. Helen Piwnica-Worms (Washington University School of Medicine). Paclitaxel and leptomycin B were purchased from Sigma. Trichostatin A was a gift from Dr. Michael Lea (UMDNJ, Newark, NJ).

To generate myc-tagged Crk II and Crk I, we utilized a pEF-BOS-myc-Rho plasmid previously provided by Dr. Naoki Katoh (Kyoto University, Japan). For construction, pEBB Crk I and pEBB Crk II were doubly digested with *Bam*HI and *Not*I (New England Biolabs) for 2 h at 37 °C, after which the doubly digested pEF-BOS-myc-Rho was CIP treated for 1 h at 37 °C and agarose gel purified. After ligation, with Crk I or Crk II DNA, pEF-BOS-myc-Crk I and pEF-BOS-myc-Crk II DNA were transformed into bacteria and grown on ampicillin-containing LB agar plates. The presence of Myc was confirmed by transfection and Western blotting with a Myc-specific antibody.

To construct a nuclear targeting mutant of Crk II, we cloned Crk-nuc upstream of the GFP reporter. The Crk-nuc contains the sequence DPKKKRKVDPKKKRKVDPKKKRKVGSTGSR C-terminal to the 3-end of the Crk II gene. To generate GFP-Crk-nuc, we PCR amplified Crk II, using the forward primer 5′TCACGGGCTAGCATGGCCGGGCAGTTC3′ and the reverse primer 5′GGTGGCGACCGGTAGGCTGAAGTCCTCATC3′. To generate the W170K-SH3(N) mutation in the GFP-Crk-nuc plasmid, PCR was performed using the primers mentioned above and pEBB W170K Crk II as a template. The ligated DNA was selected on the basis of ampicillin resistance, after which positive inserts were confirmed for the presence of Crk II by doubly digesting the DNA as well as by transfecting cells and Western blotting to check for protein expression.

To clone the linker SH3(C) region of Crk II (aa 190−305) in pNAC-PK, PCR was performed using the forward primer 5′TCACGGGATATCAAGTGTAGACCTTCC3′, and the reverse primer used was 5′CGGTGACTCGAGGCTGAAGTCCTCATC3′. The purified PCR product and pNAC-PK-myc plasmid were doubly digested using restriction enzymes *Xho*I and *Eco*RV. The ligated DNA was selected on the basis of ampicillin resistance, after which positive inserts were confirmed as described above.

Nuclear Extract Preparation. To prepare isolated nuclei, HeLa S3 cells were grown to confluency on 10 cm tissue culture dishes and harvested in PBS using a scraper. The cells were pelleted by spinning at 800*g* for 5 min at 4 °C. The cells were resuspended in 3−5 pcv (packed cell volume) of hypotonic buffer (10 mM Hepes, 1.5 mM $MgCl_2$, 10 mM KCl, 0.2 mM PMSF, 0.5 mM DTT, pH 7.9) and washed two times in this buffer. The washed cell pellet was incubated in hypotonic lysis buffer for 10 min and homogenized using a type B pestle with 8−10 strokes. The homogenate was then centrifuged at 3300*g* for 15 min at 4 °C. The supernatant obtained is the cytoplasmic fraction, and the pellet contained the intact nuclei. The nuclear pellet was washed with hypotonic buffer twice and then resuspended in $^1/_2$ pcv of low salt buffer (20 mM Hepes, 1.5 mM $MgCl_2$, 0.02 M KCl, 0.2 mM EDTA, 0.2 mM PMSF, 0.5 mM DTT, 25% glycerol, pH 7.9) by pipetting. Following this step, $^1/_2$ pcv of high salt buffer (20 mM Hepes, 1.5 mM $MgCl_2$, 1.2 M NaCl, 0.2 mM EDTA, 0.2 mM PMSF, 0.5 mM DTT, 25% glycerol, pH 7.9) was added dropwise while gently stirring the nuclear suspension, and then the mixture was incubated on a nutator at 4 °C. After 30 min incubation, insoluble debris was removed by centrifugation at 13000 rpm for 30 min at 4 °C. The supernatant was collected, which is the nuclear extract.

Immunostaining. For indirect immunofluorescence, cells were cultured and transfected on 12 mm circular poly(D-lysine)-coated coverslips (0.13−0.17 mm thick; BD Biosciences). Cells were fixed with 3% paraformaldehyde in PBS for 10 min at room temperature and then were permeabilized in 0.2% Triton X-100 in PBS for 5 min at room temperature, washed in PBS, and blocked in 50 mM glycine in PBS for 10 min. The coverslips were washed and incubated in either wash buffer (control) or primary antibody at a dilution of 1:100−1:400 for 1 h at room temperature and then washed three times in PBS−gelatin and stained with fluorescein-conjugated secondary antibody at a concentration of 1:100 (Jackson Immunologicals) for 1 h at room temperature and costained with Hoechst 33258 (Sigma) for nuclei or rhodamine-conjugated phalloidin (Molecular Probes) for actin filaments. Coverslips were mounted on a glass slide in prolong anti-fade mounting solution (Molecular Probes) to avoid photobleaching. Images were captured with a SPOT RT color CCD camera and accompanying software (Diagnostic Instruments) attached to a Nikon Eclipse TE300 microscope.

Western Blotting. Western blotting was performed following SDS−PAGE transfer to polyvinylidene difluoride (PVDF) membranes (Millipore). Blots were blocked in a 5% nonfat dry milk solution made up in TBS. Blots were subsequently incubated with appropriate primary antisera for 1 h at room temperature. The membranes were washed three times for 10 min each in TBS solution containing 0.05% Tween-20 solution. Subsequently, secondary antibodies conjugated to horseradish peroxidase (Jackson Immunologicals) were added and incubated at room temperature for 1 h. Blots were developed with an enhanced chemiluminescence kit (Perkin-Elmer).

Immunoprecipitation. Cells from confluent dishes were lysed in 400 μL of 1% HNTG buffer [20 mM Hepes (pH 7.4), 150 mM NaCl, 1% Triton X-100, 10% glycerol] or Sigma buffer (50 mM Tris-HCl, pH 7.4, 150 mM NaCl, 1 mM EDTA, 1% Triton X-100) supplemented with 1 mM sodium orthovanadate, 1 mM sodium molybdate, 1 mM PMSF, and aprotinin (5 μg/mL, final concentration) and incubated on ice for 10 min, and the insoluble material was pelleted by centrifugation at 16000*g* for 10 min at 4 °C. Protein concentrations of lysates were determined by using the Bio-Rad Bradford protein assay dye. Cell lysates (300 μg of total protein per sample) were incubated with 1.4 μg of anti-Crk antibody for 2 h at 4 °C with gentle agitation and collected by adding 25 μL of protein A−Sepharose beads and incubated for 1 h at 4 °C. The resin with bound proteins was pelleted by brief centrifugation, and the lysate was removed by aspiration. The resin was subsequently washed four times in 0.1% Triton X-100 HNTG buffer or Sigma buffer. Bound proteins were eluted by boiling in SDS−PAGE sample buffer and resolved by SDS−PAGE, with one-half of the total immunoprecipitated material loaded on the gel.

Cell Cycle Analysis. Cells (5×10^5) were trypsinized and harvested in PBS. The cells were pelleted by centrifugation at 2000 rpm for 2 min. After the cells were washed in PBS, they were fixed in ice-cold 70% ethanol for 1 h at 4 °C. Fixed cells were washed in PBS twice and resuspended in 500 μL of staining solution (10 μg/mL RNase A and 50 μg/mL propidium iodide in PBS). The samples were incubated for 30 min at 4 °C in the dark. FACS analysis was performed, and the percentage of cells in different phases of the cell cycle was assessed using ModFit V 3.0 software.

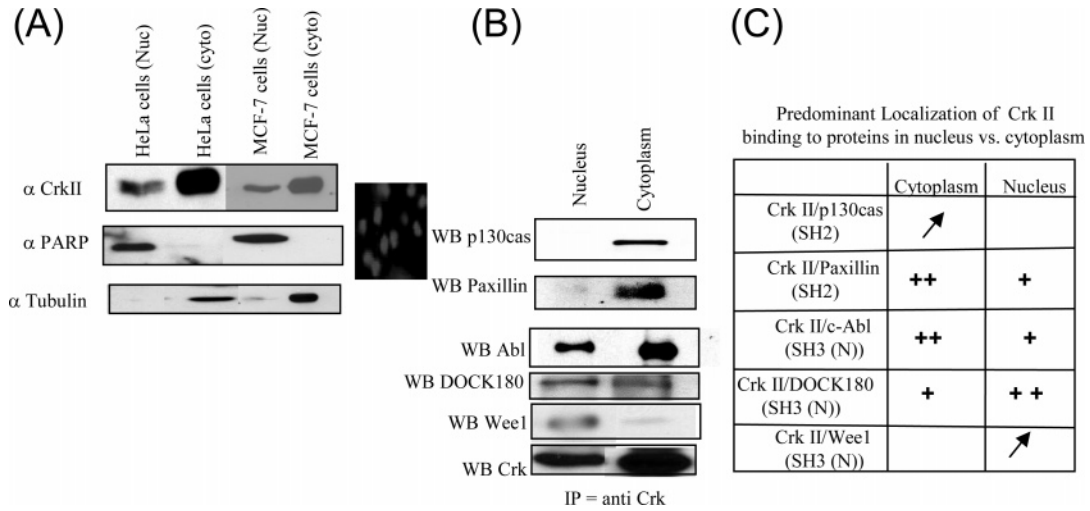

FIGURE 1: Crk II localizes in both the nucleus and cytoplasm in mammalian cells. (A) HeLa S3 cells and MCF-7 cells were fractionated to yield nuclear and cytoplasmic fractions as described in the Materials and Methods. Lysates (25 μg) were normalized, resolved by 10% SDS−PAGE, immunoblotted with anti-Crk II RF51 antisera, and then stripped and reprobed with anti-PARP antibody and anti-tubulin antibody to verify the purity of the nuclear and cytoplasmic fraction. After the nuclear pellet was obtained, an aliquot was washed and stained with Hoechst 33258 to show the intact nuclear membrane (insert). (B) HeLa S3 cells were fractionated, and the nuclear and cytoplasmic lysates (400 μg) were normalized for protein and subjected to immunoprecipitation with anti-Crk II antibody. The immune complexes were collected with prewashed protein A−Sepharose beads, and the bound proteins were resolved on a 10% SDS−PAGE and immunoblotted with the indicated antibodies (p130^{cas}, paxillin, Abl, DOCK180 and Wee1). Similar results were obtained with MCF-7 cells. (C) The relative enrichment of these complexes in the nucleus vs cytoplasm is summarized. (++) indicates that the pool was enriched in this fraction, and (↑) indicates a virtual complete localization in that fraction.

UV Irradiation. Prior to irradiation, cells were washed with PBS prewarmed to 37 °C. Then the PBS was removed, and the cells were irradiated using a UV-C lamp emitting 254 nm UV light (40 μJ/cm^2) while the control plates were left outside the incubator without media or PBS for the same length of time required for irradiation of the plates. Immediately after irradiation, the same conditioned medium was added back to avoid any serum stimulation, to both the irradiated and control plates. The cells were incubated at 37 °C for 4 h before being harvested.

Apoptosis Assay. Cells (5×10^5) were grown in 60 mm tissue culture dishes. The cells were transfected with LT1 (Mirus) reagent as described above. Apoptotic and necrotic cells were assessed using the Annexin V-PE apoptosis detection kit I from BD Pharmigen, and the assay was performed as per the manufacturer's protocol.

Cell Spreading Assay. NIH 3T3 (5×10^4) cells were grown in a six-well culture dish. After 24 h of transfection, the cells were trypsinized and counted. Ten thousand cells were plated on fibronectin-coated coverslips for 20 min at 37 °C. The cells were washed in PBS twice and then fixed in 3% paraformaldehyde for 30 min at room temperature. Following fixation the cells were permeabilized in 0.02% Triton X-100 solution for 5 min at room temperature. Cells were then stained with Hoechst 33258 for nuclei and rhodamine−phalloidin for actin at room temperature for 10 min. For visualization under the microscope, coverslips were mounted in anti-fade solution (Molecular Probes).

RESULTS

Nuclear Expression of Crk II. Crk II and Crk L proteins are expressed in both cytosolic and nuclear compartments. Using biochemical fractionation of native unstimulated mammalian cells to obtain purified nuclei, we estimate that between 5% and 10% of the total endogenous Crk II resides in the nucleus, and this was independent of the cell type investigated including HEK 293T, HeLa cells, MCF-7, or NIH 3T3 cells (Figure 1A and data not shown). Isolated washed nuclei were stained with DAPI to show that their nuclear membranes were intact and not ruptured (Figure 1A insert), and the purity of the cytoplasmic and nuclear fractions was assayed by immunoblotting with tubulin (a cytoplasmic marker) (*43*) and PARP (a nuclear-specific marker) (*44*). To assess whether cytosolic and nuclear compartments contained distinct protein complexes, we prepared cytosolic and nuclear fractions (normalized for total cellular protein) and performed immunoprecipitation with anti-Crk antisera followed by Western blot analysis against several known Crk binding proteins, including p130^{cas}, paxillin, Abl, DOCK180, and Wee1 (*45*). In native unstimulated cells, complexes of Crk with the cytoskeletal proteins, paxillin and p130^{cas}, which interact with the SH2 domain of Crk through pYDHP sequences in the targets (*46*−*49*), were predominantly in the cytosolic compartment, whereas Crk-Abl and Crk-DOCK180 were in both compartments (Figure 1B). Surprisingly, in the case for Crk II-Wee1 and Crk II-DOCK180, these complexes were predominantly detected in the nucleus.

To explore the mechanism of Crk II translocation under steady-state conditions, we generated epitope-tagged Crk proteins by fusing Crk II, Crk I, or mutants to a C-terminal GFP or an N-terminal myc peptide epitope tag. As shown in Figure 2A−C, Crk II retains its ability to partition in the cytosol and nucleus when modestly overexpressed in HeLa or NIH 3T3 cells. In contrast, Crk I, which is functionally analogous to v-Crk (*4*), was only localized in the cytosolic fraction, and this was confirmed using indirect immunofluoresence (Figure 2B). Because Crk II contains no obvious NLS, translocation is likely to occur indirectly, via a complex with Abl, DOCK180, Wee1, or another binding protein that shuttles between the nuclear and cytoplasmic compartments.

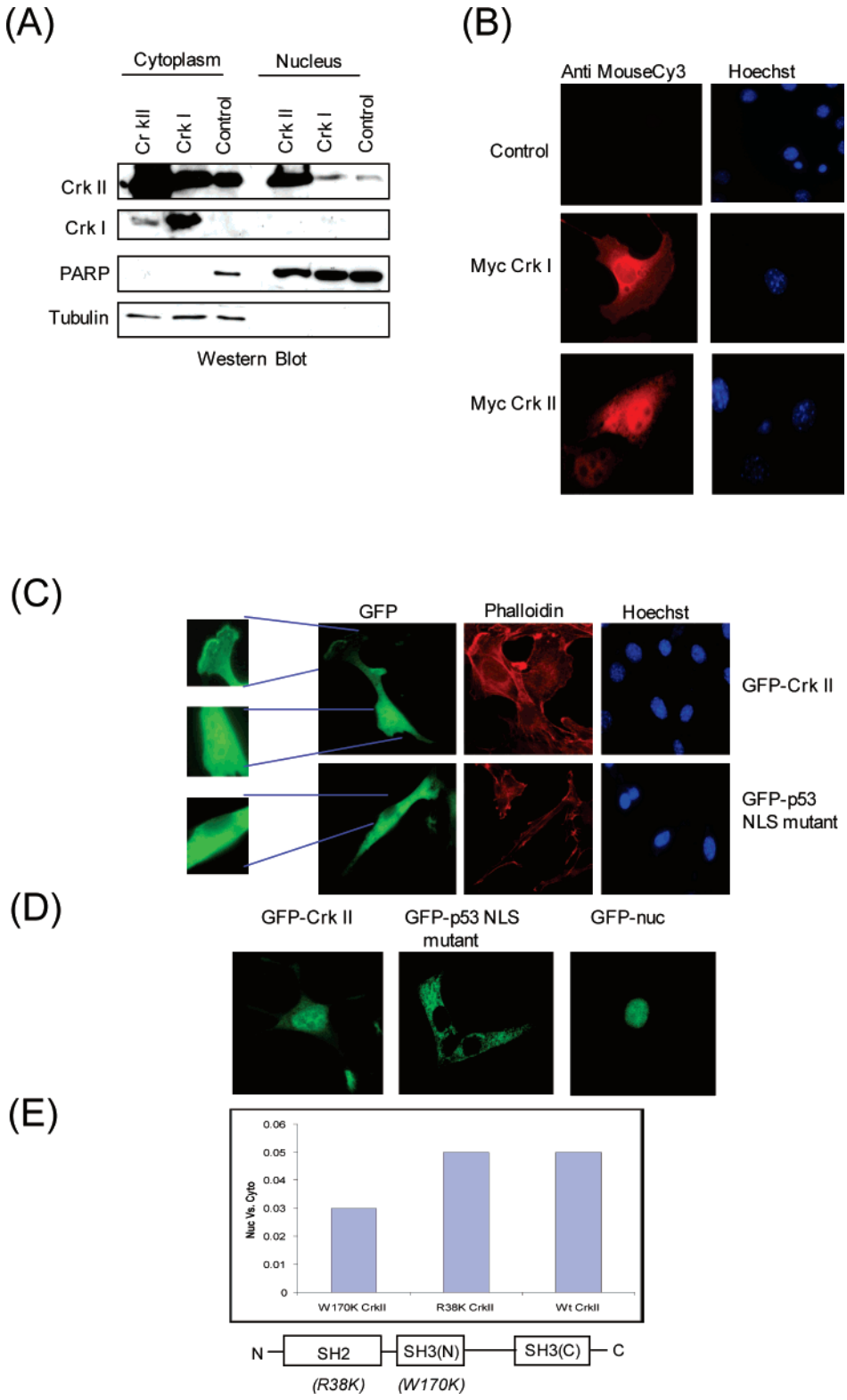

FIGURE 2: Indirect immunofluorescence and confocal microscopic analysis of Crk II localization. (A) HeLa cells were transfected with 0.5 μg of plasmids of pEBBCrk I or pEBBCrk II. After 24 h, cells were subjected to subcellular fractionation as in Figure 1. The lysates (25 μg) were resolved on 12% SDS−PAGE and immunoblotted with RF51 antibody, which recognizes both Crk I and Crk II. The blots were stripped and reprobed with anti-PARP antibody and anti-tubulin antibody. (B) Indirect immunofluoresence analysis of Crk II and Crk I expression. NIH 3T3 cells were transfected with 0.5 μg of pEF-BOS-Crk I-myc or pEF-BOS-Crk II-myc expression plasmid, and after 24 h Crk-expressing cells were fixed in 3% paraformaldehyde and immunostained with anti-Myc 9E10 antibody or counterstained by Hoechst 33258. (C) NIH 3T3 cells were cultured on 12 mm diameter coverslips and transfected with 0.5 μg of expression plasmids for GFP-Crk II or GFP-p53 NLS mutant. After 24 h, the cells were fixed and counterstained for rhodamine−phalloidin and Hoechst 33258 for 10 min to determine the actin filaments and nuclei, respectively. (D) In panel D, cells were transfected as in (C), except that confocal microscopy was used to section the nuclear plane. (E) NIH 3T3 cells stably expressing WT Crk II, R38K Crk II, or W170K Crk II were grown in G418-containing media. The stably expressing WT Crk II and the mutants were subjected to nuclear and cytosolic fractionation. Densitometric analysis was performed on the Western blot and plotted in a graphical format.

This has been well illustrated for Crk L, which binds tyrosine-phosphorylated STAT5 or the estrogen receptor which facilitates ligand-dependent nuclear translocation (*36*, *50*). Shown in Figure 2C,D are immunofluoresence (Figure 2C) and confocal microscopy (Figure 2D) images of NIH 3T3 cells expressing GFP fusion proteins of Crk. GFP-Crk II was expressed at both lamellipodia at the plasma membrane as well as in the nucleus (Figure 2C insert). Indirect immunofluorescence with a Crk II-specific antibody also revealed nuclear localization in NIH 3T3 cells (data not shown). As a negative control, we transfected cells with the GFP p53 NLS mutant (*51*), which has a point mutation within the NLS sequence of p53 protein and has been shown previously to lack nuclear localization (Figure 2C,D). GFP fused in frame to repetitive nuclear localization sequences of SV40 (GFP-nuc) had an entirely nuclear localization (Figure 2D), suggesting this construct can be used to drive cellular proteins into the nucleus (see below). Moreover, to investigate the domain requirement that underlies Crk II nuclear localization, we stably expressed R38K Crk II (SH2 domain mutant) and the W170K Crk II [SH3(N) domain mutant] in NIH 3T3 cells. These mutant forms of Crk II have been previously characterized to block the ability of Crk II to form protein complexes. When NIH 3T3 cells stably expressing Crk II and the mutant forms were fractionated, although no single domain mutant completely abrogated nuclear localization, expression of W170K Crk II showed more exclusion compared to the SH2 domain mutants (Figure 2E), suggesting that binding of SH3(N) to proline-containing target proteins may be one of the principal mechanisms directing nuclear uptake.

Functionality of the Putative NES Sequence in Crk II SH3-(C). Previous studies identified a LALEVGELVKV sequence in the C-terminal SH3 domain with broad homology to a NES. Studies by Smith et al. indicated this sequence regulates nuclear export via Crm1-dependent binding (*41*). Although previous studies by our laboratory indicated that the NES was buried in the hydrophobic core of the SH3(C) (Figure 3D), more recent studies have demonstrated that the NES in Crk L may become unmasked by monomer−dimer transition and exposed to regulate nuclear export (*42*). To explore the physiological role of the NES in more detail, we treated cells with leptomycin B (LMB). LMB inhibits the export receptor Crm1, and hence when cells are treated with LMB, cargo protein cannot be exported and accumulates in the nucleus (*52*). As a positive control, we compared cells expressing GFP-Crk II to cells expressing a recombinant GFP-nuc-nes protein (Figure 3A,B). GFP-nuc-nes is an engineered construct containing three NLS from SV40 large T-antigen and the NES from PKR inhibitor (PKI) fused to GFP (Figure 3A). Following LMB treatment, GFP-nuc-nes rapidly accumulated in the nucleus whereas, under similar conditions, no change in GFP-Crk II localization was noted (Figure 3B). Moreover, using coimmunoprecipitation and GST pull-down studies with the isolated GST SH3(C) or GST linker SH3-(C) of Crk II, we failed to observe stable interaction between Crk II and Crm 1 in HEK 293T cell lysates (Figure 3C). Although these studies failed to find evidence for a functional NES, it remains to be observed whether under specialized circumstances Crk II nuclear localization becomes leptomycin sensitive.

Because Crk II, but not Crk I, localized to the nucleus, we wanted to test whether the SH3(C) domain or SH3 linker region might have an as yet unrealized nuclear localization signal. To test this directly, we cloned the linker and SH3-(C) in frame downstream to the C-terminus of the cytoplasmic protein, pyruvate kinase (Figure 3E). Pyruvate kinase is a glycolytic enzyme shown to only localize in the cytoplasm of mammalian cells (*53*, *54*). However, as shown in Figure 3F, when NIH 3T3 cells were transfected with either myc-Wee1 (as a positive control) or myc-pyruvate kinase or myc-pyruvate kinase-linker-SH3(C), the latter resulting proteins were exclusively cytoplasmic. Collectively, these results indicate that the linker-SH3(C) of Crk II is not a major regulatory element for Crk II translocation to the nucleus, and under steady-state conditions Crk II localization does not possess LMB sensitivity.

Nuclear Targeting of Crk with SV40 Large T-Antigen NLS. Assignment of function to the nuclear pool of Crk II is complicated by a preeminent pool of cytoplasmic Crk II. Hence, to better study the function of nuclear Crk II independent of its cytoplasmic function, we designed a targeted cassette to drive Crk II into the nucleus. We fused three NLS motifs from the SV40 large T-antigen in frame to the C-terminus of Crk II (this protein product will be referred to as GFP-Crk-nuc hereafter) [Figure 4A (i)]. Overexpression of GFP-Crk-nuc was verified by preparing lysates and Western blotting [Figure 4A (ii)]. We also confirmed the GFP-Crk-nuc localization to the nucleus by direct immunofluorescence when transfected in NIH 3T3 cells (Figure 4B). Interestingly, when we attempted to generate stable GFP-Crk-nuc- expressing cells during selection in G418, GFP-Crk-nuc-expressing cells became less and less numerous over time and could not be propagated in multiple independent clones. Flow cytometric analysis (24−72 h) indicated that over time the number of GFP-expressing cells decreased posttransfection (Figure 5A), and in examining the protein profile we observed that the GFP-Crk-nuc protein also was unstable during a similar time frame (Figure 5B). This was not due to GFP nuclear expression, since GFP-nuc-expressing cells could be propagated in G418. As shown in Figure 5C, flow cytometric analysis of the cells after 11 days of G418 selection also revealed similarly that the GFP-Crk-nuc cells were less numerous over time.

Due to the inability to generate stable GFP-Crk-nuc-expressing cell lines during G418 selection, we used transiently transfected cells and FACS sorting to purify and analyze GFP-expressing cells. Forty-eight hours after transfection, GFP control and GFP-Crk-nuc-expressing cells were FACS sorted and analyzed in terms of their ability to bind to fibronectin and proliferate after replating compared to non-GFP-expressing cells. Sorting resulted in over 90% purification in GFP-, GFP-Crk-, and GFP-Crk-nuc-enriched cells (Figure 6A). After collection, cells were either replated on tissue culture dishes for up to 24 h or lysed immediately for assessment of G2/M cell cycle parameters. GFP and GFP-Crk II cells readily replated and adhered to the tissue culture dishes when observed microscopically after 24 h, while GFP-Crk-nuc cells were characteristically poorly adherent and most of the cells failed to adhere (data not shown). Furthermore, when we cultured FACS-sorted GFP-Crk-nuc-expressing cells in high serum overnight, these cells did not show phosphohistone H3 phosphorylation (a measure of

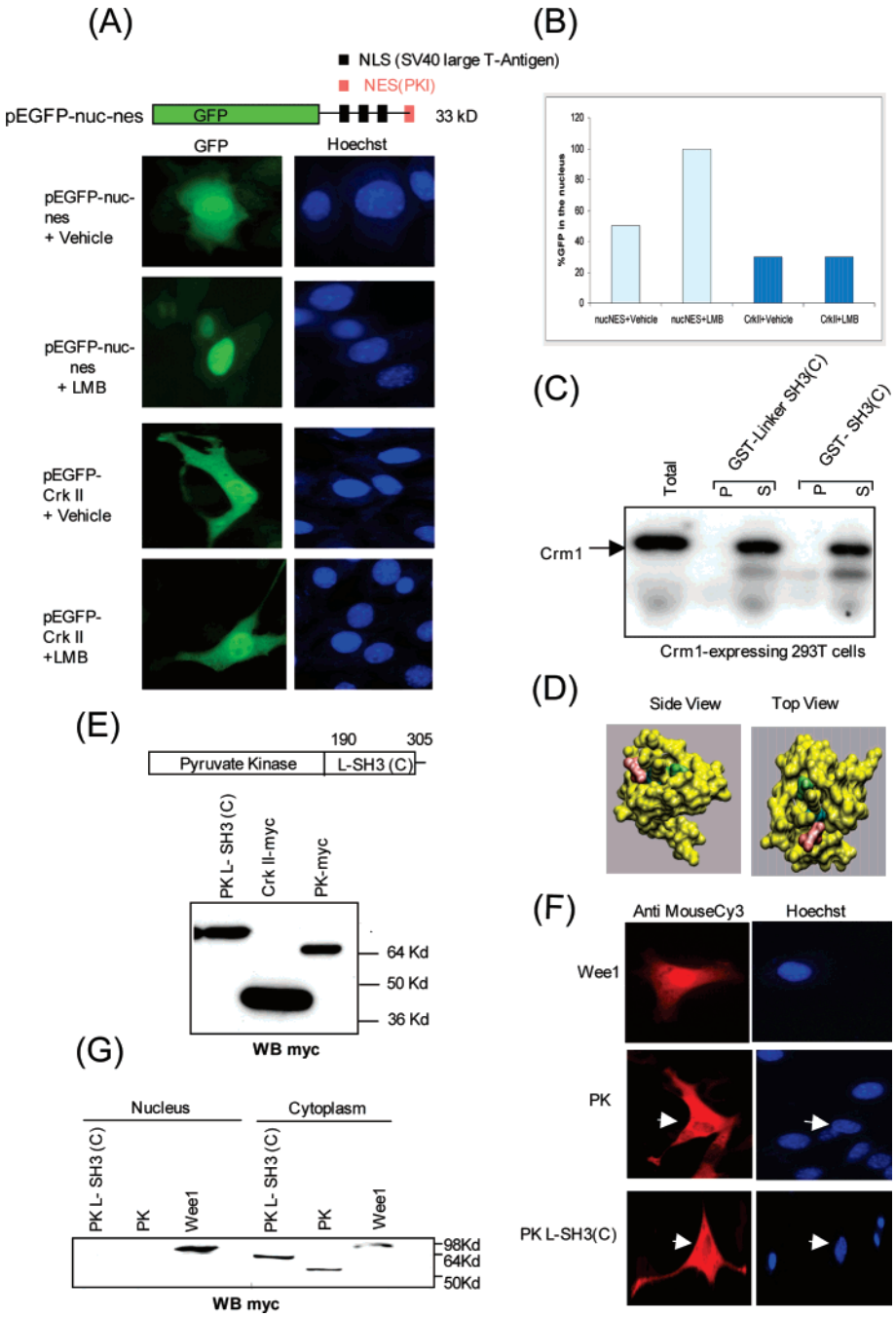

FIGURE 3: Effect of leptomycin B and the role of the SH3(C) in Crk II nuclear localization. (A) pEGFP-nuc-nes was used as a positive control for LMB sensitivity. The GFP fusion protein has 3 NLS from the SV40 large T-antigen and 1 NES derived from PKI (PKR inhibitor). NIH 3T3 cells grown on 10 mm coverslips were transfected with 0.5 μg of either GFP-nuc-nes or GFP-Crk II. 24 h posttransfection, cells were treated with 10 ng/mL LMB for 30 min or vehicle (ethanol), after which they were fixed and stained with Hoechst 33258 to observe nuclear sequestration of GFP-Crk II or GFP-nuc-nes. (B) A quantification of the results before and after LMB treatment is shown graphically. (C) Binding of Crk II proteins to Crm1. HEK 293T cells were transfected with plasmid expressing Crm1. 48 h posttransfection the cells were lysed in a 1% HNTG detergent buffer. Purified recombinant GST-SH3(C) or GST-linker-SH3(C) (5 μg) was added to 25 μL of prewashed GSH−Sepharose beads and gently rocked for 2 h at 4 °C. GST proteins bound to GSH−Sepharose beads were added to Crm1 expressing cell lysate and rocked for a further 1 h at 4 °C. Binding of proteins (P) versus the soluble fraction (S) was assayed by collecting the fractions bound to GSH−Sepharose beads, and they were resolved on a 10% SDS−PAGE and immunoblotted for Crm1. (D) Homology modeling of the C-terminal SH3 domain using the minimal energy molecular modeling program Look (version 3.5) was employed using the crystal structure of mouse Crk SH3(N) bound to an interacting peptide as the template. The top and side views of the model are shown. Note that the critical valine residue depicted in purple required for Crm1 binding is buried inside the hydrophobic pocket. (E) The SH3(C) domain does not drive nuclear localization. The pNAC-pyruvate kinase myc-tagged linker SH3(C) or SH3(C) of Crk II was cloned downstream of pyruvate kinase as described in the Materials and Methods. After transfection, detergent lysates were prepared to determine protein expression (lower panel). In panel F, indirect immunofluorescence staining in NIH 3T3 cells was done after overexpressing 0.5 μg of PK or PK linker SH3(C) or Wee1 plasmid using a Myc-specific antibody. The cells were then incubated with anti-mouse-CY3 conjugated secondary antibody and Hoechst 33258. (G) 0.5 μg of PK-myc, Crk II-myc, or PK L-SH3(C) plasmid DNA was transfected in HEK 293T cells. Cells were lysed in sigma buffer, and protein expression of the cloned protein was detected by Western blotting with a Myc antibody. The cells were fractionated, and the nuclear and cytoplasmic lysates were normalized for protein. 25 μg of cell lysates was immunoblotted with anti-Myc to detect the localization of the transfected proteins.

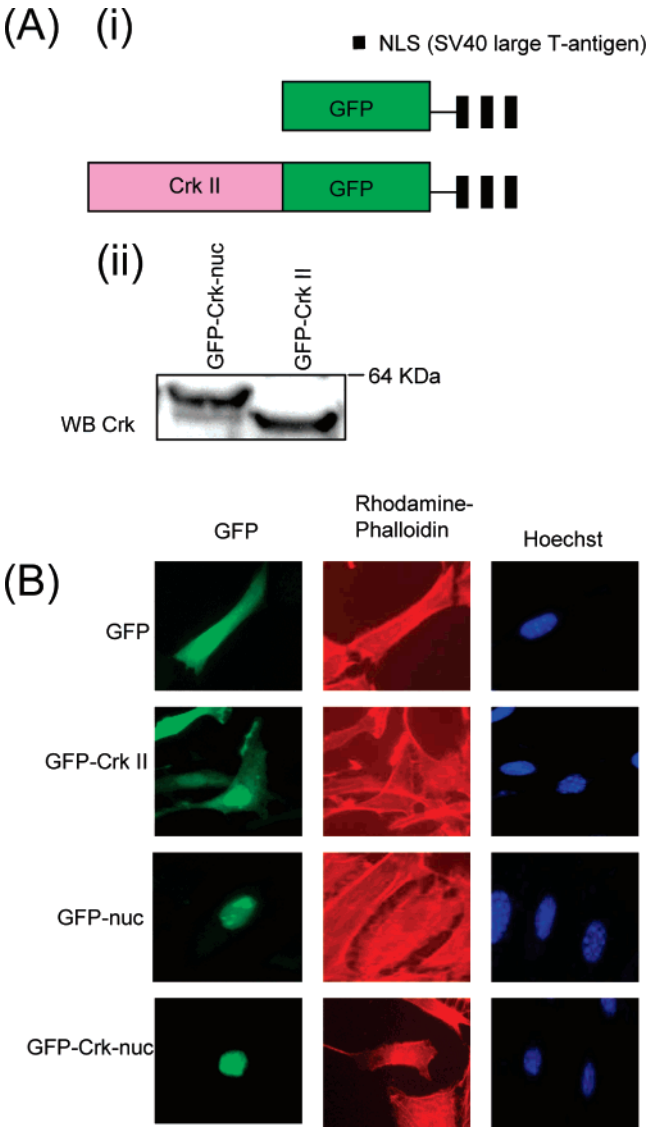

FIGURE 4: Generation of a nuclear Crk II targeting cassette. (A) (i) Schematic representation of the structure of pEGFP-nuc used in these experiments. Solid boxes indicate NLS from SV40 large T-antigen. (ii) HEK 293T cells were transfected with 0.5 μg of either GFP-Crk II or GFP-Crk-nuc. Cells were lysed in Sigma buffer, and the protein expression of GFP-Crk-nuc was confirmed by immunoblotting with anti-Crk II antibody. (B) 0.5 μg of GFP, GFP-Crk II, GFP-nuc, or GFP-Crk-nuc plasmid DNA was transfected in NIH 3T3 cells. Indirect immunofluorescence microscopy shows that GFP-Crk-nuc has persistent and durable nuclear expression.

successful mitosis) (Figure 6B). These data suggested to us that GFP-Crk-nuc cells were either G2/M arrested or undergoing apoptosis.

Crk II Binds to Wee1 without Inducing a G2/M Block. We were attracted to the possibility that GFP-Crk-nuc might induce a G2/M arrest based on the previous observations that Crk II binds to the G2/M regulatory protein Wee1 (*40*). However, we first wanted to confirm the interaction between Wee1 and Crk II in our system. Consistent with reports of Smith et al., we noted stable interaction between Wee1 and Crk II in the nucleus (Figure 1B). As shown in Figure 7B, pull downs of detergent lysates with GST-Crk II resulted in stable binding of Crk II to Wee1.

After confirming the interaction between Wee1 and Crk II in mammalian cells, we investigated the effect of Crk II on Wee1 activity by coexpressing Wee1 with GFP-Crk II or GFP-Crk-nuc proteins (Figure 7A). For example, if Crk II binding to Wee1 activated Wee1 kinase activity, we might expect increased Tyr^{15} Cdc2 phosphorylation and a G2/M blockage, since Cdc2 is directly phosphorylated by Wee1. However, expression of GFP-Crk-nuc did not increase Cdc2-Tyr^{15} phosphorylation. Treatment of cells with nocodazole, a known G2/M blocking drug (*55*, *56*), decreased Cdc2-Tyr^{15} phosphorylation and served as a control for these experiments. Additionally, when we examined the DNA content by PI staining of GFP-Crk-nuc cells compared to GFP-Crk II-expressing cells, these cells did not show significant changes in G2/M in the cell cycle profile (Figure 7C). Treatment of cells with paclitaxel (*57*) or trichostatin A (*58*) was used as a control that shows the integrity of G2/M and G1/S check points, respectively, in HeLa cells (Figure 7C). These data suggest that the interaction between Crk II and Wee1 may occur independently of the cell cycle regulatory capabilities of Wee1.

Nuclear Crk II Causes Spontaneous Apoptosis and Potentiates UV-Mediated Apoptosis. We investigated the effect of GFP-Crk-nuc on cell spreading on fibronectin-coated coverslips. As shown in Figure 8A, unlike GFP-Crk II, GFP-Crk-nuc-expressing cells failed to spread on fibronectin surfaces, and the nuclei were pycnotic. Hence, we next explored the ability of GFP-Crk-nuc to induce apoptosis by analyzing whether GFP-Crk-nuc induced PARP cleavage or was positive for apoptosis by annexin V staining. PARP is a substrate of Caspase-3, which becomes cleaved by activated Caspase 3 to generate a fragment of 85 kDa from the 110 kDa parent protein (*59*). As shown in Figure 8B (i), expression of GFP-Crk II showed a reproducible enhancement in the extent of apoptosis assessed by both phosphatidylserine externalization (from 11−23% for GFP-Crk versus GFP-Crk-nuc expressing cells) and PARP cleavage 48 h posttransfection compared to GFP-expressing cells. Expression of GFP-Crk-nuc enhanced the extent of apoptosis, suggesting this localization of Crk II makes cells more prone to apoptosis.

To assess the more immediate influences of Crk II, we next investigated the ability of Crk II to induce apoptosis as well as potentiate a proapoptotic signal. Toward this goal, we treated cells with low level UV to induce a delayed apoptotic response. Treatment of cells with low level UV causes a time-dependent translocation of Crk II to the nucleus as a function of apoptosis (apoptosis assessed by PARP cleavage products) (Figure 8C). To explore whether Crk II caused or potentiated UV-mediated apoptosis, we next expressed GFP, GFP-Crk II, GFP-Crk-nuc, or GFP-W170K-Crk-nuc in HeLa cells and after 48 h subjected them to UV irradiation with 40 μJ/cm^2 and cultured them for a further 4 h. As shown in Figure 8B (ii), expression of GFP-Crk-nuc also potentiated the effects of low dose UV irradiation compared to GFP-Crk II cells. Expression of the SH3(N) domain mutant (GFP-W170K-Crk-nuc) induced less apoptosis when cells were UV irradiated, suggesting that this effect requires Crk protein−protein interactions. Taken together, these results suggest that nuclear Crk II may sensitize cells to proapoptotic signals and this pool of Crk II antagonizes the cytoplasmic pool.

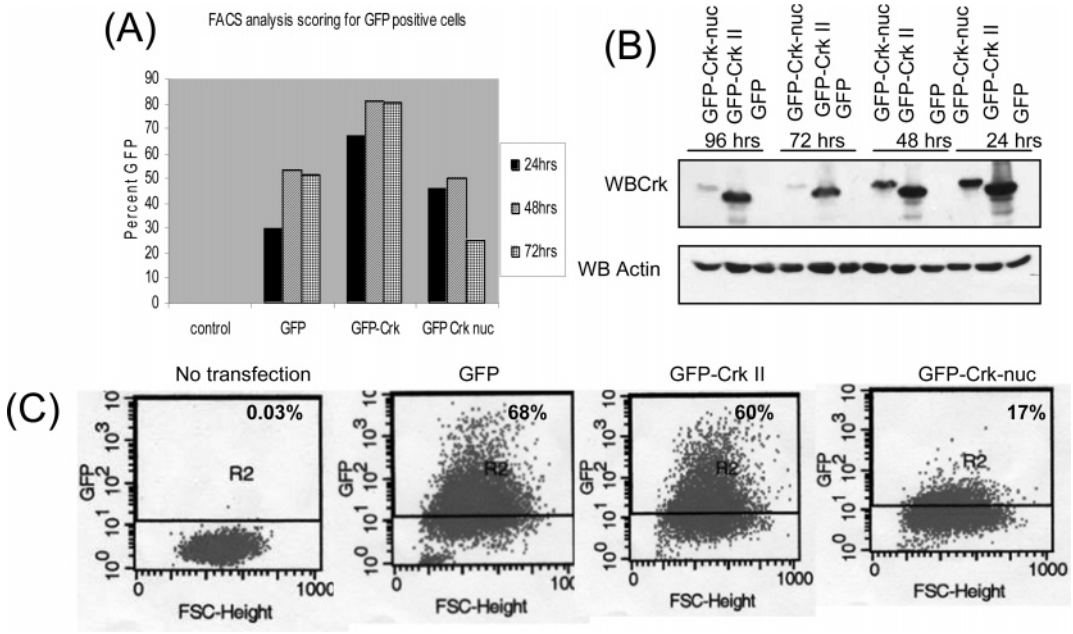

FIGURE 5: GFP-Crk-nuc expressing cells are unstable to drug selection. (A) Plasmid DNA expressing GFP, GFP-Crk II, or GFP-Crk-nuc was transfected into HEK 293T cells in triplicate. After 24, 48, or 72 h of transfection, the culture medium was washed, and the cells were harvested in PBS. The GFP intensity was then measured using FACS immediately, and the average of the percentage of GFP-positive cells was plotted in a graph. (B) Concomitantly, cells were lysed in Sigma buffer, and total cellular protein (15 μg) was blotted with a Crk antibody. The blot was stripped and reprobed with actin antibody to show uniform loading. (C) HeLa cells were transfected with 1 μg of GFP, GFP-Crk II, and GFP-Crk-nuc plasmid, and then the cells were cultured in G418 containing media. After 11 days the cells were trypsinized and harvested in PBS. The percent of GFP-expressing cells in each plate was scored using FACS analysis.

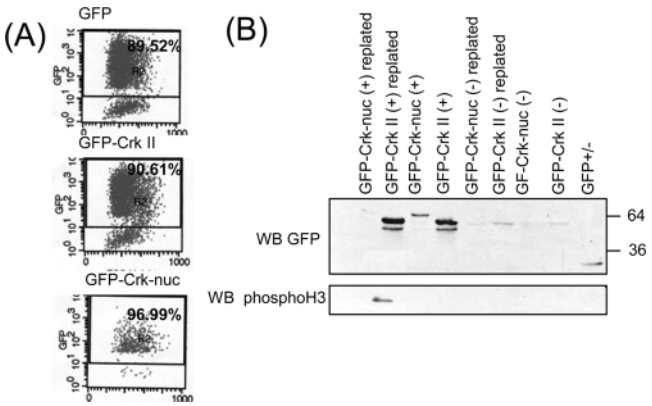

FIGURE 6: FACS purification to obtain GFP-expressing cells. (A) HeLa cells were transfected with 1 μg of GFP, GFP Crk II, or GFP-Crk-nuc plasmid DNA. 48 h posttransfection, the cells were trypsinized and harvested in PBS containing 5 mM EDTA solution and processed for cell sorting to separate the GFP-expressing cells. (+) depicts the transfected and (−) depicts the nonsorted pool of HeLa cells. (B) The GFP-expressing cells obtained from cell sorting were counted, and 2×10^5 cells were lysed in RIPA buffer immediately or 2×10^5 cells were replated on tissue culture dishes. After 24 h the replated cells were observed under the microscope, and both the floating and adherent cells were collected and lysed in RIPA buffer. The lysates were normalized for protein, and 25 μg of total protein was immunoblotted with anti-GFP. The blot was stripped and reprobed with anti-phosphohistone H3 to monitor mitosis.

DISCUSSION

Previous studies have shown that Crk II and Crk L proteins are localized in both cytoplasmic and nuclear compartments. For example, following ligand stimulation of various hematopoietic cells, Crk L binds to tyrosine-phosphorylated STAT5, and subsequently a STAT5/Crk L complex translocates into the nucleus to transactivate IFN-regulatory response elements (*32*, *36*). Moreover, studies in fibroblasts showed that ionizing radiation induces association of Wee1 and Crk II in the nucleus, which has subsequently been implicated in inducing apoptosis (*41*). Finally, recent studies also indicate that Crk II and Crk L proteins have putative nuclear export sequences and bind Crm1 (*41*, *42*). We undertook this study to better characterize the nuclear function of Crk II. Toward this goal, we targeted Crk II exclusively to the nucleus by fusing GFP-Crk II to tandem nuclear localization signals from the SV40 large T-antigen. Persistent and durable nuclear localization decreased cell adhesion and induced spontaneous apoptosis. Our data are consistent with an emerging model in which Crk II undergoes cytoplasmic-nuclear shuttling as a molecular switch to regulate cell adhesion, survival, and apoptosis. We posit that shifting the pools of Crk II to favor a cytosolic localization would promote survival, while shifting the pools toward nuclear Crk II would promote apoptosis. Consistent with this idea, following UV irradiation, we noted an increase in the nuclear pool of Crk II, suggesting the cytosolic to nuclear balance is shifted during apoptosis.

The factors that regulate Crk II nuclear translocation are still not well understood. On the basis of studies here, we favor the idea that Crk II translocation is mediated by protein complexes involving the SH3(N) domain. One relevant candidate is Abl since nuclear and cytoplasmic localizations of Abl have distinct effects on apoptosis. Activation of cytoplasmic Abl and Crk Tyr222 phosphorylation has been implicated in promoting apoptosis (*60*−*63*). In such a model, activation of cytoplasmic Abl may play an indirect role in apoptosis, by inactivating a "pro-survival" pathway transmitted by engaged $p130^{cas}$/Crk/DOCK180. Additionally, activation of nuclear Abl causes apoptosis induced from a variety of signals, such as chemotherapeutic drugs, ionizing radia-

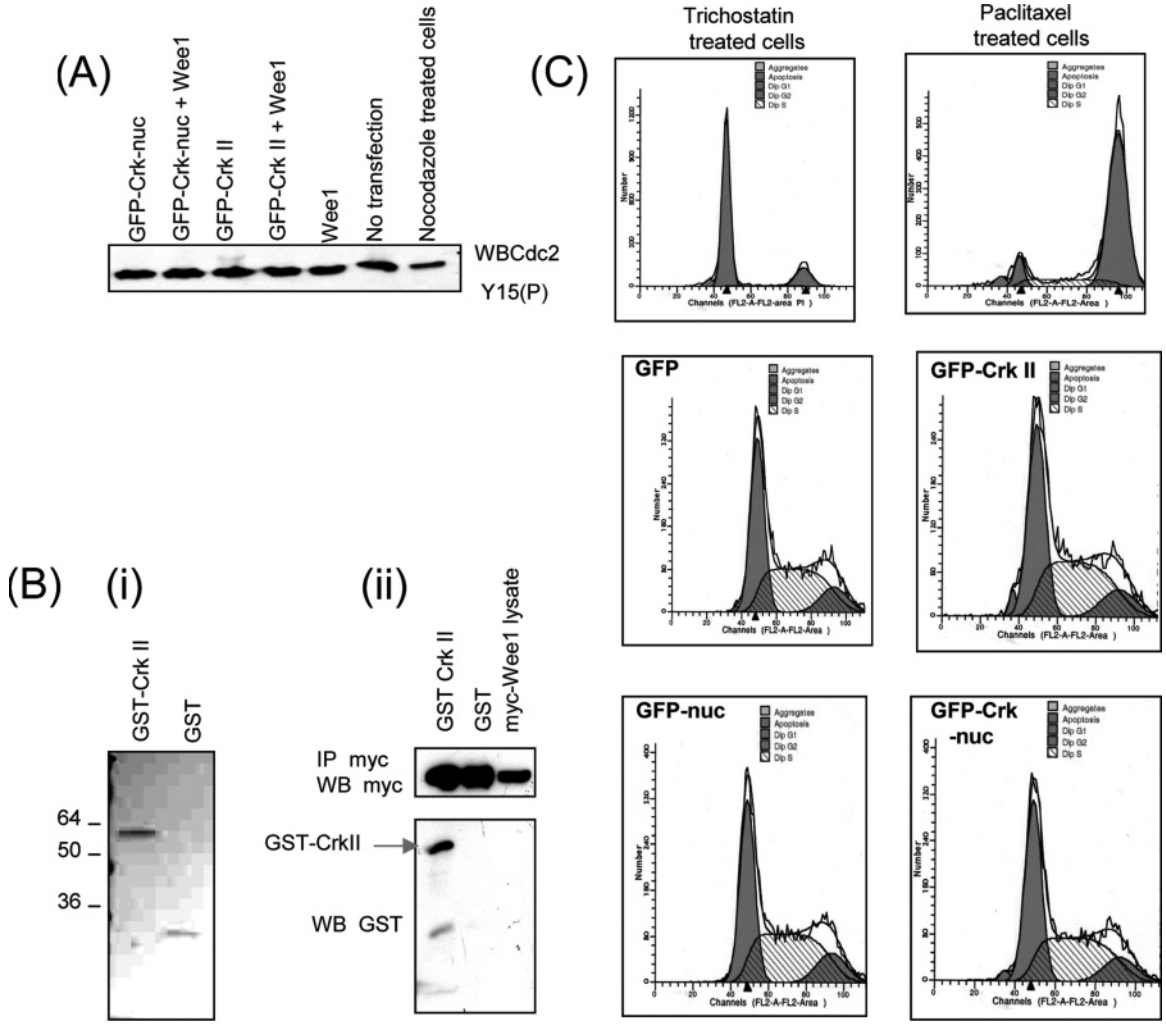

FIGURE 7: Wee1−Crk II interaction and effect on the G2/M phase of the cell cycle. (A) HeLa cells were transfected with 0.5 μg of Wee1 alone or along with 0.5 μg of GFP-Crk II or 0.5 μg of GFP-Crk-nuc plasmid DNA. Cells were lysed in Sigma buffer and immunoblotted for phospho Cdc2Y15, an indicator of Wee1 kinase activity. Control lysates were made from cells treated with nocodazole for 16 h. (B) (i) Coomassie staining of purified GST or GST-Crk II proteins. (ii) 0.5 μg of Wee1 was overexpressed in HEK 293T cells. Wee1 was immunoprecipitated with 1.7 μg of Myc antibody, and either GST or GST-Crk II purified recombinant proteins were added to the immune complexes. The proteins bound to Wee1 were resolved on a SDS−PAGE and immunoblotted with anti-GST antibody. The blot was stripped and reprobed with Myc antibody to assess Wee1 immunoprecipitation. (C) Cell cycle profile of GFP-, GFP-Crk II-, GFP-nuc-, or GFP-Crk-nuc-expressing cells were measured by FACS based on DNA content measurement by propidium iodide staining. HeLa cells were transfected with 1 μg of GFP, GFP-Crk II, GFP-nuc, or GFP-Crk-nuc with at least 80−90% transfection efficiency. Following 48 h of transfection the cells were ethanol fixed, stained with propidium iodide, and analyzed using FACS. HeLa cells were either treated with trichostatin (G1 block) or paclitaxel (M phase) to show that the G1 and G2/M checkpoints in HeLa cells are intact. The FACS data were analyzed using the MOD-FIT program.

tion, and TNF-α (*64*). Abl shuttles back and forth between the nucleus and the cytoplasm depending on the availability of the NLS versus NES of Abl, and during apoptosis there may be a dysregulation of these processes. For example, c-Abl translocates into the nucleus in response to DNA damage or oxidative stress, resulting from the phosphorylation of Abl and 14-3-3, the net result is unmasking of the NLS in Abl and nuclear translocation (*65*, *66*). Cells that lack c-Abl or express kinase-inactive forms of Abl show resistance to radiation and drug-induced apoptosis, suggesting that nuclear activation of Abl is necessary to evoke a proapoptotic signal, although the exact target of nuclear Abl activation is not clear. In addition, cytoplasmic Abl has two caspase cleavage sites at Asp565 and Asp958. The cleavage of this latter Asp958 site would produce an interesting protein product, in which the kinase domain, the Crk binding domain, the three NLS, and the DNA binding domain remain intact, whereas the extreme C-terminal NES is cleaved (*67*). Recent studies with activated Bcr-Abl showed treatment with LMB enhanced nuclear accumulation and resulted in apoptosis in human CML cells (*68*). Further studies are required to ascertain whether Abl-mediated Crk phosphorylation or Crk-mediated Abl transactivation in the nucleus contributes to a proapoptotic event.

We also noted stable interactions between Crk II and nuclear DOCK180 and Wee1. DOCK180 is an important guanine nucleotide exchange factor that stabilizes the high-energy nucleotide-free transition state as Rac1 cycles from a GDP- to GTP-bound state (*69*). Presently, there are 11 members in the DOCK superfamily of proteins (*70*). However, not all of the members belonging to this superfamily possess the PxxPxK/R motif that could interact with the SH3(N) domain of Crk, which indicates that DOCK may have both Crk-dependent and Crk-independent functions (*71*)

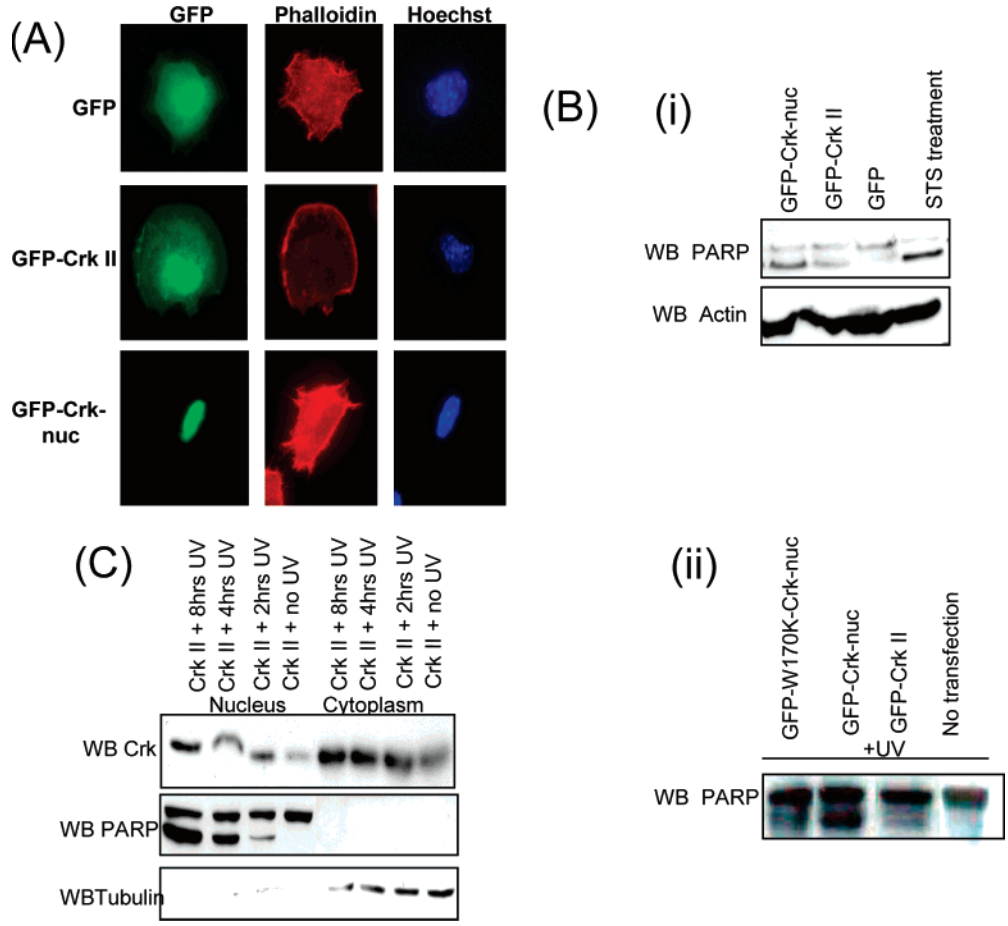

FIGURE 8: GFP-Crk-nuc-expressing cells have a reduced ability to spread on a fibronectin-coated surface and induce apoptosis in cells. (A) NIH 3T3 cells were transfected with 0.5 μg of either GFP-Crk II or GFP-Crk-nuc expression plasmid. Following 24 h, the cells were trypsinized, and 5×10^4 cells were seeded on fibronectin coverslips for 20 min, fixed with 3% paraformaldehyde for 30 min at room temperature, permeabilized with 0.2% Triton X-100 solution, and counterstained with rhodamine−phalloidin and Hoechst 33825. (B) (i) PARP cleavage in lysates from GFP-, GFP-Crk II-, or GFP-Crk-nuc-expressing cells. HeLa cells were transfected with 1 μg of GFP, GFP-Crk II, or GFP-Crk-nuc. 48 h posttransfection the cells were lysed in Sigma buffer, and 25 μg of lysate was immunoblotted with anti-PARP antibody. The blot was stripped and reprobed with anti-actin for loading control. STS (staurosporine) treatment for 4 h was used to induce apoptosis in HeLa cells. Lysates from STS-treated cells were used as a positive control for PARP cleavage. (ii) HeLa cells were transfected with 1 μg of GFP-Crk II, GFP-Crk-nuc, or GFP-W170K-Crk-nuc expression plasmids. 48 h posttransfection the cells were UV-C irradiated for 4 h as described in the Materials and Methods. The cells were lysed in sigma buffer and immunoblotted with anti-PARP antibody. (C) HeLa cells were transfected with pEBB WT Crk II expression plasmid. 48 h posttransfection the cells were irradiated with UV for 5 min and incubated for a further 2, 4, and 8 h. The cells were fractionated after the indicated time periods, and immunoblotting was performed with a Crk II antibody. The blot was stripped and reprobed with anti-PARP to assess purity of the nuclear fraction as well as to monitor apoptosis. Note that PARP cleavage was increased with an increase in duration of UV irradiation. The blot was reprobed with anti-tubulin to check the purity of the nuclear fraction.

Although DOCK 180 has an evolutionarily conserved cytoplasmic function in cell migration and phagocytosis of apoptotic cells, other studies have noted that a significant pool of DOCK180 is nuclear (*72*). However, the role of the nuclear DOCK180−Crk II complex awaits further investigation, as well as the specific homologues of DOCK that are relevant for Crk II binding.

Wee1 encodes a nuclear kinase that prevents mitotic entry by tyrosine phosphorylation-mediated inactivation of p34cdc2 (*73*). Activation of Wee1 protects cells from DNA damage and mitotic catastrophes by blocking cells in the G2/M phase of the cell cycle (*74*, *75*). Interestingly, later studies showed that a Wee1−Crk II complex (presumably in the nucleus) could trigger apoptosis, and these studies pointed to the subcellular localization of Crk as a primary regulatory event that underscores apoptosis. Consistent with the results of Kornbluth and colleagues, we noted a stable interaction between Crk II and Wee1 in HEK 293T and HeLa cells, as well as through GST pull-down experiments in detergent lysates. We originally hypothesized that Crk II binding to Wee1 might cause a G2/M block, and despite observing a stable complex of Crk II and Wee1 in the nucleus, we did not observe G2/M block nor did Crk II appear to increase Tyr^{15} phosphorylation of Cdc-2 when coexpressed with Wee1.

Another important question is whether nuclear Crk II can be exported back out of the nucleus, and if so, can apoptosis be aborted? Presently, the answer to this question is not known, but recent data suggest that Crk II can be directly transported out of the nucleus via binding to the NES chaperone protein Crm1 in an energy-dependent process. Although this NES motif is partially buried in the hydrophobic core of the domain [in a region of Crk SH3(C) that is considered very stable], interesting studies by Feller and colleagues suggest this motif (their studies were performed with Crk L) may become accessible during monomer to

dimer transition (*42*). For example, binding of Crk II to one or more of these proteins might lead to regulated dimerization, or alternatively, phosphorylated Crk might bind in trans to the SH2, in addition to the intramolecular Crk SH2−Crk Y221 phosphotyrosine interaction. This could be a pretext for efficient Crk II binding and nuclear transport. In this study, we did not find that subcellular localization of Crk wild-type or the C-terminal portion of Crk fused to pyruvate kinase was sensitive to leptomycin B, a fungal metabolite that binds to and inactivates Crm1. One possible interpretation of this result may be that Crk dimerization is subject to a tight, but unknown regulatory signal. It is of obvious importance to determine when and how Crk II may undergo monomer−dimer transition as recently reported.

In summary, we found that targeted expression of Crk II to the nucleus with NLS sequences from SV40 caused spontaneous apoptosis. We also found that GFP-Crk-nuc-expressing cells were impaired in spreading on adhesion-coated surfaces. This would suggest that Crk stoichiometrically titrates signaling effects in the integrin pathway into a functional buffered cellular compartment. Such an idea would be consistent with the idea of nuclear compartmentalization as a negative strategy, possibly as a way to "store" protein complexes in an inert manner. On the other hand, it is equally plausible that Crk II actively participates in the apoptotic cascade by interacting with Abl, Wee1, or DOCK180 within the nucleus. Further characterization of this nuclear fraction and the identification of relevant binding proteins should help to better define the function of nuclear Crk II.

ACKNOWLEDGMENT

We thank Sally Kornbluth (Duke University) and Helen Piwnica-Worms (Washington University School of Medicine) for sharing reagents. We also thank Kamalendra Singh for assistance with the homology modeling of the SH3(C) of Crk II.

REFERENCES

1. Feller, S. M., et al. (1998) Physiological signals and oncogenesis mediated through Crk family adapter proteins, *J. Cell. Physiol. 177*, 535−552.
2. Mayer, B. J., Hamaguchi, M., and Hanafusa, H. (1988) A novel viral oncogene with structural similarity to phospholipase C, *Nature 332*, 272−275.
3. Tsuchie, H., et al. (1989) A newly isolated avian sarcoma virus, ASV-1, carries the crk oncogene, *Oncogene 4*, 1281−1284.
4. Matsuda, M., et al. (1992) Two species of human CRK cDNA encode proteins with distinct biological activities, *Mol. Cell. Biol. 12*, 3482−3489.
5. Reichman, C. T., et al. (1992) The product of the cellular crk gene consists primarily of SH2 and SH3 regions, *Cell Growth Differ. 3*, 451−460.
6. ten Hoeve, J., et al. (1993**)** Isolation and chromosomal localization of CRKL, a human crk-like gene, *Oncogene 8*, 2469−2474.
7. Imaizumi, T., et al. (1999) Mutant mice lacking Crk-II caused by the gene trap insertional mutagenesis: Crk-II is not essential for embryonic development, *Biochem. Biophys. Res. Commun. 266*, 569−574.
8. Guris, D. L., et al. (2001) Mice lacking the homologue of the human 22q11.2 gene CRKL phenocopy neurocristopathies of DiGeorge syndrome, *Nat Genet. 27*, 293−298.
9. Birge, R. B., et al. (1993) Identification and characterization of a high-affinity interaction between v-Crk and tyrosine-phosphorylated paxillin in CT10-transformed fibroblasts, *Mol. Cell. Biol. 13*, 4648−4656.
10. Feller, S. M., Knudsen, B., and Hanafusa, H. (1995) Cellular proteins binding to the first Src homology 3 (SH3) domain of the proto-oncogene product c-Crk indicate Crk-specific signaling pathways, *Oncogene 10*, 1465−1473.
11. Law, S. F., et al. (1996) Human enhancer of filamentation 1, a novel p130cas-like docking protein, associates with focal adhesion kinase and induces pseudohyphal growth in *Saccharomyces cerevisiae*, *Mol. Cell. Biol. 16*, 3327−3337.
12. Vuori, K., et al. (1996) Introduction of p130cas signaling complex formation upon integrin-mediated cell adhesion: a role for Src family kinases, *Mol. Cell. Biol. 16*, 2606−2613.
13. Takai, S., et al. (1994) Mapping of the human C3G gene coding a guanine nucleotide releasing protein for Ras family to 9q34.3 by fluorescence in situ hybridization, *Hum. Genet. 94*, 549−550.
14. Tanaka, S., et al. (1994) C3G, a guanine nucleotide-releasing protein expressed ubiquitously, binds to the Src homology 3 domains of CRK and GRB2/ASH proteins, *Proc. Natl. Acad. Sci. U.S.A. 91*, 3443−3447.
15. Knudsen, B. S., Feller, S. M., and Hanafusa, H. (1994) Four proline-rich sequences of the guanine-nucleotide exchange factor C3G bind with unique specificity to the first Src homology 3 domain of Crk, *J. Biol. Chem. 269*, 32781−32787.
16. Feller, S. M., Knudsen, B., and Hanafusa, H. (1994) c-Abl kinase regulates the protein binding activity of c-Crk, *Embo J. 13*, 2341−2351.
17. Garcia-Guzman, M., et al. (1999) Met-induced JNK activation is mediated by the adapter protein Crk and correlates with the Gab1-Crk signaling complex formation, *Oncogene 18*, 7775−7786.
18. Girardin, S. E., and Yaniv, M. (2001) A direct interaction between JNK1 and CrkII is critical for Rac1-induced JNK activation, *EMBO J. 20*, 3437−3446.
19. Kodama, H., et al. (2003) Selective involvement of p130Cas/Crk/Pyk2/c-Src in endothelin-1-induced JNK activation, *Hypertension 41*, 1372−1379.
20. Mochizuki, N., et al. (2000**)** Crk activation of JNK via C3G and R-Ras, *J. Biol. Chem. 275*, 12667−12671.
21. Tanaka, S., Ouchi, T., and Hanafusa, H. (1997) Downstream of Crk adaptor signaling pathway: activation of Jun kinase by v-Crk through the guanine nucleotide exchange protein C3G, *Proc. Natl. Acad. Sci. U.S.A. 94*, 2356−2361.
22. Tanaka, S., and Hanafusa, H. (1998) Guanine-nucleotide exchange protein C3G activates JNK1 by a ras-independent mechanism. JNK1 activation inhibited by kinase negative forms of MLK3 and DLK mixed lineage kinases, *J. Biol. Chem. 273*, 1281−1284.
23. Leng, J., et al. (1999) Potentiation of cell migration by adhesion-dependent cooperative signals from the GTPase Rac and Raf kinase, *J. Biol. Chem. 274*, 37855−37861.
24. Reiske, H. R., et al. (1999) Requirement of phosphatidylinositol 3-kinase in focal adhesion kinase-promoted cell migration, *J. Biol. Chem. 274*, 12361−12366.
25. Klemke, R. L., et al. (1998) CAS/Crk coupling serves as a "molecular switch" for induction of cell migration, *J. Cell Biol. 140*, 961−972.
26. Miller, C. T., et al. (2003) Increased C-CRK proto-oncogene expression is associated with an aggressive phenotype in lung adenocarcinomas, *Oncogene 22*, 7950−7957.
27. Linghu, H., et al. (2006) Involvement of adaptor protein Crk in malignant feature of human ovarian cancer cell line MCAS, *Oncogene 25*, 3547−3556.
28. Watanabe, T., et al. (2006) Adaptor molecule Crk is required for sustained phosphorylation of Grb2-associated binder 1 and hepatocyte growth factor-induced cell motility of human synovial sarcoma cell lines, *Mol. Cancer Res. 4*, 499−510.
29. Reichman, C., et al. (2005) Transactivation of Abl by the Crk II adapter protein requires a PNAY sequence in the Crk C-terminal SH3 domain, *Oncogene 24*, 8187−8199.
30. Angers-Loustau, A., et al. (1999) Protein tyrosine phosphatase-PEST regulates focal adhesion disassembly, migration, and cytokinesis in fibroblasts, *J. Cell Biol. 144*, 1019−1031.
31. Noren, N. K., et al. (2006) The EphB4 receptor suppresses breast cancer cell tumorigenicity through an Abl-Crk pathway, *Nat. Cell Biol. 8*, 815−825.
32. Rhodes, J., et al. (2000) CrkL functions as a nuclear adaptor and transcriptional activator in Bcr-Abl-expressing cells, *Exp. Hematol. 28*, 305−310.
33. Fish, E. N., et al. (1999) Activation of a CrkL-stat5 signaling complex by type I interferons, *J. Biol. Chem. 274*, 571−573.
34. Lekmine, F., et al. (2002) The CrkL adapter protein is required for type I interferon-dependent gene transcription and activation of the small G-protein Rap1, *Biochem. Biophys. Res. Commun. 291*, 744−750.

35. Oda, A., et al. (2000) Thrombopoietin and interleukin-2 induce association of CRK with STAT5, *Biochem. Biophys. Res. Commun. 278*, 299−305.
36. Ota, J., et al. (1998) Association of CrkL with STAT5 in hematopoietic cells stimulated by granulocyte-macrophage colony-stimulating factor or erythropoietin, *Biochem. Biophys. Res. Commun. 252*, 779−786.
37. Ozaki, K., et al. (1998) Thrombopoietin induces association of Crkl with STAT5 but not STAT3 in human platelets, *Blood 92*, 4652−4662.
38. Evans, E. K., et al. (1997) Crk is required for apoptosis in *Xenopus* egg extracts, *EMBO J. 16*, 230−241.
39. Kornbluth, S. (1997) Apoptosis in *Xenopus* egg extracts, *Methods Enzymol. 283*, 600−614.
40. Smith, J. J., et al. (2000) Wee1-regulated apoptosis mediated by the crk adaptor protein in *Xenopus* egg extracts, *J. Cell Biol. 151*, 1391−1400.
41. Smith, J. J., et al. (2002) Apoptotic regulation by the Crk adapter protein mediated by interactions with Wee1 and Crm1/exportin, *Mol. Cell. Biol. 22*, 1412−1423.
42. Harkiolaki, M., et al. (2006) The C-terminal SH3 domain of CRKL as a dynamic dimerization module transiently exposing a nuclear export signal, *Structure. 14*, 1741−1753.
43. Willingham, M. C., Yamada, S. S., and Pastan, I. (1980) Ultrastructural localization of tubulin in cultured fibroblasts, *J. Histochem. Cytochem. 28*, 453−461.
44. Schreiber, V., et al. (1992) The human poly(ADP-ribose) polymerase nuclear localization signal is a bipartite element functionally separate from DNA binding and catalytic activity, *EMBO J. 11*, 3263−3269.
45. Feller, S. M. (2001) Crk family adaptors-signalling complex formation and biological roles, *Oncogene 20*, 6348−6371.
46. Schaller, M. D., and Schaefer, E. M. (2001) Multiple stimuli induce tyrosine phosphorylation of the Crk-binding sites of paxillin, *Biochem. J. 360* (Part 1), 57−66.
47. Turner, C. E. (1998) Paxillin, *Int. J. Biochem. Cell Biol. 30*, 955−959.
48. Turner, C. E. (2000) Paxillin interactions, *J. Cell Sci. 113* (Part 23), 4139−4140.
49. Valles, A. M., Beuvin, M., and Boyer, B. (2004) Activation of Rac1 by paxillin-Crk-DOCK180 signaling complex is antagonized by Rap1 in migrating NBT-II cells, *J. Biol. Chem. 279*, 44490−44496.
50. Nautiyal, J., Kumar, P. G., and Laloraya, M. (2004) 17Beta-estradiol induces nuclear translocation of CrkL at the window of embryo implantation, *Biochem. Biophys. Res. Commun. 318*, 103−112.
51. Akakura, S., et al. (2001) A role for Hsc70 in regulating nucleocytoplasmic transport of a temperature-sensitive p53 (p53Val-135), *J. Biol. Chem. 276*, 14649−14657.
52. Kudo, N., et al. (1998) Leptomycin B inhibition of signal-mediated nuclear export by direct binding to CRM1, *Exp. Cell Res. 242*, 540−547.
53. Gali, P. (1979) Epithelial localization of pyruvate kinase L (ATP pyruvate phosphotransferase EC 2.7.1.40) in rat liver, *C.R. Seances Acad. Sci. D 289*, 1029−1032.
54. Gali, P., et al. (1980) Localization of pyruvate kinase M1 (ATP pyruvate phosphotransferase-2.7.1.40) in nervous tissue of the rat. Preliminary results, *C.R. Seances Acad. Sci. D 290*, 1533−1536.
55. Harper, J. V. (2005) Synchronization of cell populations in G1/S and G2/M phases of the cell cycle, *Methods Mol. Biol. 296*, 157−166.
56. Hayne, C., Tzivion, G., and Luo, Z. (2000) Raf-1/MEK/MAPK pathway is necessary for the G2/M transition induced by nocodazole, *J. Biol. Chem. 275*, 31876−31882.
57. Jordan, M. A., et al. (1996) Mitotic block induced in HeLa cells by low concentrations of paclitaxel (Taxol) results in abnormal mitotic exit and apoptotic cell death, *Cancer Res. 56*, 816−825.
58. Kim, Y. B., et al. (2000) Mechanism of cell cycle arrest caused by histone deacetylase inhibitors in human carcinoma cells, *J. Antibiot. (Tokyo) 53*, 1191−1200.
59. Bernardi, R., et al. (1995) Activation of poly(ADP-ribose)-polymerase in apoptotic human cells, *Biochimie 77*, 378−384.
60. Barila, D., et al. (2003) Caspase-dependent cleavage of c-Abl contributes to apoptosis, *Mol. Cell. Biol. 23*, 2790−2799.
61. Kawai, H., Nie, L., and Yuan, Z. M. (2002) Inactivation of NF-kappaB-dependent cell survival, a novel mechanism for the proapoptotic function of c-Abl, *Mol. Cell. Biol. 22*, 6079−6088.
62. Yoshida, K., and Miki, Y. (2005) Enabling death by the Abl tyrosine kinase: mechanisms for nuclear shuttling of c-Abl in response to DNA damage, *Cell Cycle 4*, 777−779.
63. Kain, K. H., Gooch, S., and Klemke, R. L. (2003) Cytoplasmic c-Abl provides a molecular 'Rheostat' controlling carcinoma cell survival and invasion, *Oncogene 22*, 6071−6080.
64. Wang, J. Y. (2000) Regulation of cell death by the Abl tyrosine kinase, *Oncogene 19*, 5643−5650.
65. Pendergast, A. M. (2005) Stress and death: breaking up the c-Abl/14-3-3 complex in apoptosis, *Nat. Cell Biol. 7*, 213−214.
66. Yoshida, K., et al. (2005) JNK phosphorylation of 14-3-3 proteins regulates nuclear targeting of c-Abl in the apoptotic response to DNA damage, *Nat. Cell Biol. 7*, 278−285.
67. Holcomb, M., et al. (2006) Deregulation of proteasome function induces Abl-mediated cell death by uncoupling p130CAS and c-CrkII, *J. Biol. Chem. 281*, 2430−2440.
68. Aloisi, A., et al. (2006) BCR-ABL nuclear entrapment kills human CML cells: ex vivo study on 35 patients with the combination of imatinib mesylate and leptomycin B, *Blood 107*, 1591−1598.
69. Kiyokawa, E., et al. (1998) Activation of Rac1 by a Crk SH3-binding protein, DOCK180, *Genes Dev. 12*, 3331−3336.
70. Cote, J. F., and Vuori, K. (2002) Identification of an evolutionarily conserved superfamily of DOCK180-related proteins with guanine nucleotide exchange activity, *J. Cell Sci. 115* (Part 24), 4901−4913.
71. Tosello-Trampont, A. C., et al. (2007) Identification of two signaling submodules within the CrkII/ELMO/Dock180 pathway regulating engulfment of apoptotic cells, *Cell Death Differ. 14*, 963−972.
72. Yin, J., et al. (2004) Nuclear localization of the DOCK180/ELMO complex, *Arch. Biochem. Biophys. 429*, 23−29.
73. Piwnica-Worms, H., et al. (1991) p107wee1 is a serine/threonine and tyrosine kinase that promotes the tyrosine phosphorylation of the cyclin/p34cdc2 complex, *Cold Spring Harbor Symp. Quant. Biol. 56*, 567−576.
74. Feilotter, H., et al. (1992) Regulation of the G2-mitosis transition, *Biochem. Cell Biol. 70*, 954−971.
75. Parker, L. L., and Piwnica-Worms, H. (1992) Inactivation of the p34cdc2-cyclin B complex by the human WEE1 tyrosine kinase, *Science 257*, 1955−1957.

BI700537E